CONFORMATIONAL DYNAMICS OF THE ENZYME-SUBSTRATE COMPLEX OF PROTEIN KINASE A WITH PSEUDOSUBSTRATE SP20 AND ADENOSINE TRIPHOSPHATE

T.I. Mulashkina[1]*, M.S. Leonova[1,2], M.G. Khrenova[1,3]

[1]Chemistry Department, Lomonosov Moscow State University,
1/3 Leninskie Gory, Moscow, 119991 Russia; *e-mail: mulashkinati@my.msu.ru
[2]Emanuel Institute of Biochemical Physics of Russian Academy of Sciences,
4 Kosygina str., Moscow, 119334 Russia
[3]Bach Institute of Biochemistry, Federal Research Centre "Fundamentals of Biotechnology"
of the Russian Academy of Sciences, 33 Leninsky ave., Moscow, 119071 Russia

The phosphorylation reaction, catalyzed by the enzyme protein kinase A (PKA), plays one of the key roles in the work of the glutamatergic system, primarily involved in memory functioning. The analysis of the dynamic behavior of the enzyme-substrate complex allows one to learn the mechanism of the enzymatic reaction. According to the results of classical molecular dynamics calculations followed by hierarchical clustering, the most preferred proton acceptor during the phosphorylation reaction catalyzed by PKA is the carboxyl group of the amino acid residue Asp166; however, the γ-phosphate group of ATP can also act as an acceptor.

Key words: protein kinase A; molecular dynamics; conformations; enzyme-substrate complex; ATP

DOI: 10.18097/PBMC20247006421

INTRODUCTION

The normal activity of the central nervous system is controlled by the balance of glutamic acid (Glu) and γ-aminobutyric acid (GABA). The disruption of this balance causes many cognitive diseases, attention deficit hyperactivity disorder, increased nervousness and anxiety in adults, sleep disorders and insomnia, epilepsy. The brain glutamatergic system is the basic system of memory and learning and is responsible for maintaining this balance. Currently, the glutamatergic system is not as well studied as other brain systems. Moreover, chemical reactions with neurotransmitters and related chemical compounds catalyzed by enzymes of the system have not been sufficiently studied [1, 2].

One of the important enzymes involved in the glutamatergic system is protein kinase A (PKA). PKA catalyzes the phosphorylation reaction of the hydroxyl groups of serine or threonine in the potassium channel; this leads to the release of potassium ions (K^+) through the ion channel and to the generation of potential on the membrane [1]. In addition, phosphorylation is a therapeutic target for the treatment of many diseases including oncological, inflammatory, immune and neurodegenerative ones [3].

PKA is a heterotetramer [4] consisting of two regulatory and two catalytic subunits. The catalytic subunit consists of a small lobe (N-lobe), a large lobe (C-lobe) and a loop between them. A small lobe includes residues responsible for ATP binding, while a large lobe provides a surface for binding of phosphorytion substrates. The base of the loop between the small and large lobes forms a deep, predominantly hydrophobic pocket for the ATP adenine moiety. The enzymatic reaction occurs in this region, and it facilitates phosphate group the transfer from ATP to the substrate [5].

In the active site of PKA, Mg^{2+} ions are coordinated by ATP phosphate groups, amino acid residues and phosphorylated substrates (Fig. 1). Such metal coordination stabilizes the reactants and facilitates the phosphoryl transfer reaction. In addition, the active site contains a catalytic triad consisting of certain amino acid residues crucial for catalytic activity. The catalytic triad comprises Lys72 and Glu91 from the small lobe and Asp184 from the large lobe. These residues bind ATP and orient the phosphate groups for transfer to the protein substrate. The aspartate residue, Asp166, in the active site of PKA likely catalyzes the phosphoryl transfer reaction. These residues together play a crucial role in proton capture, nucleophilic attack, and stabilization of transition states [5–7].

The mechanism of the phosphorylation reaction can be either dissociative or associative [7]. With the associative mechanism, the nucleophilic attack occurs before the P-O bond cleavage, resulting in a pentacoordinated transition state. In the case of dissociative mechanism, the cleaving of the P-O bond precedes the formation of a bond between phosphorus and the nucleophile, therefore the transition state is metaphosphate.

An important point in the study of the phosphorylation reaction is the determination of the proton acceptor from the hydroxyl group

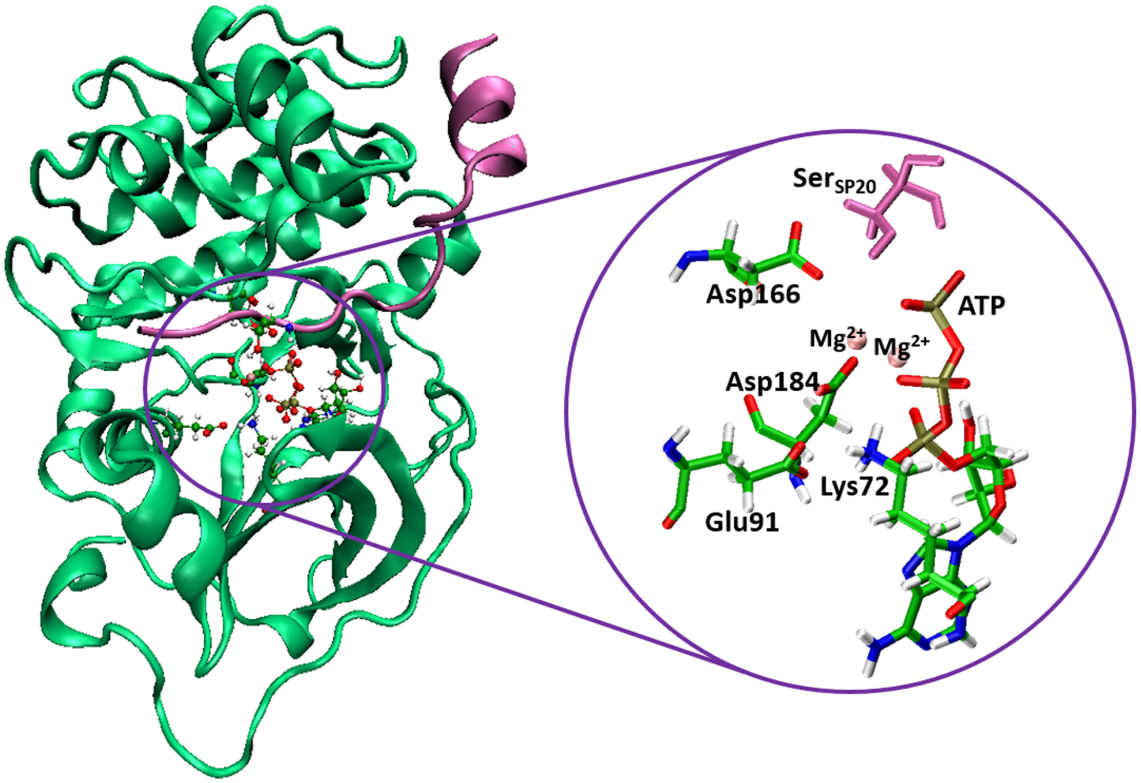

Figure 1. The PKA structure (green cartoon) with the oligopeptide pseudosubstrate SP20 (pink cartoon) is shown on the left. Key amino acid residues of the catalytic subunit, magnesium cations, ATP and a SP20 serine residue are shown on the right. Here and on the next figures carbon atoms are colored in green, oxygen atoms are shown in red, hydrogen atoms are shown in white, magnesium ions are shown in pink, phosphorus atoms are shown in orange, and nitrogen blue, respectively. The color version of the figure is available in the electronic version of the article.

of the serine substrate at the beginning of the reaction, which, in turn, determines the initial structure of the enzyme-substrate complex for modeling chemical steps. Therefore, in this work, possible conformations of the PKA active site in complex with ATP and a pseudosubstrate SP20 have been identified and compared. For this purpose, classical molecular dynamic trajectories were calculated, and subsequent hierarchical clustering was carried out. Using this approach, three conformations of the enzyme-substrate complex have been determined.

METHODS

The crystal structure of PKA in the complex with the oligopeptide pseudosubstrate SP20 (PDB ID: 4IAC) was used as an initial source for coordinates of the system [4]. In the initial structure, β,γ-methylene-ATP was changed for ATP, the phosphorylated state of the residues pSer139, pThr197, and pSer338 were preserved. Using the Reduce program [8], hydrogen atoms were added to the protein structure so that the pH of the system was 7. The protonated state of the side chains of histidine residues was determined by their local environment. The His87 residue was modeled in a positively charged protonated form, while the remaining histidine residues were modeled in a neutral form.

The enzyme-substrate complex was solvated with water molecules so that the distance from the protein atoms to the rectangular cell boundary was at least 10 Å, while four chloride anions were added to the system to neutralize the positive charge excess. The preparation of a full-atomic model of the system, as well as visualization and analysis of the structure were carried out in the VMD program [9].

Molecular dynamic (MD) modeling was carried out in two steps. During the first step, the solvation shell was relaxed using classical MD modeling in the NAMD program [10]. The CHARMM36 force field was used to describe the enzyme and pseudosubstrate [11]; CGenFF was utilized for the ATP molecule [12] and TIP3P for water molecules [13]. The length of the MD trajectory with a fixed protein and substrate atoms was 1 ns, which allowed the volume of the system to reach an equilibrium value related to the pressure of 1 atm. The size of the system was 75×73×88 Å^3. Then a series of four MD simulations of 250 ns each was carried out. Thus, 40 000 frames of the molecular dynamic trajectory were collected for analysis.

All molecular dynamics simulations were performed in the isothermal-isobaric NPT ensemble at of 298 K and a 1 atm, which were kept constant using the Langevin thermostat [14] and the Noze-Hoover barostat [15, 16], respectively; the integration time step was 1 fs.

A hierarchical clustering of molecular dynamics trajectories was performed using the TTClust tool [17] to determine the possible conformations of the protein substrate and ATP in the active site. Clustering was carried out only for molecular fragments that could directly participate in the reaction, namely ATP, the serine residue of the substrate SP20 (Ser_{SP20}) and the aspartic acid residue, Asp166, which was a putative acceptor of the proton of the hydroxyl serine group during the reaction. To do this, all trajectories were combined, and the frames were aligned over the main protein chain. RMSD was calculated between pairs of frames for selected molecular fragments. The Ward's algorithm was used for all calculations of the connection matrices [18].

RESULTS AND DISCUSSION

The results of the hierarchical clustering in the TTClust program are shown in Figure 2. Four clusters corresponding to different conformations of ATP and the residues Asp166, Ser_{SP20} with an average RMSD of 0.79 were obtained. It can be seen from the overlay of representative frames (Fig. 2B) that these clusters differ mainly in the conformation of the Ser_{SP20} of the substrate, namely, the hydroxyl group position relative to the oxygen atoms of aspartic acid residue and ATP triphosphate moiety. The most frequent conformation during dynamics is K_2, the remaining conformations occur with almost equal frequency (Fig. 2B). It can be seen from the RMSD matrix between clusters (Fig. 2A) that smaller RMSD values are observed between the K_2 and K_3 (0.60) and the K_2 and K_4 (0.47) conformations.

A detailed comparison of representative structures corresponding to different clusters is shown in Figure 3. Indeed, a comparison of K_2 and K_3 shows that these are very similar structures. In these conformations, the hydrogen atom of the the serine residue hydroxyl group is directed towards the oxygen of the γ-phosphate group, this suggests that the phosphate group oxygen the may be a proton acceptor during the reaction. In the case of K_3, the distance between the proton and the oxygen of the phosphate group is less than in the case of K_2, and a smaller nucleophilic attack distance is also observed. However, based

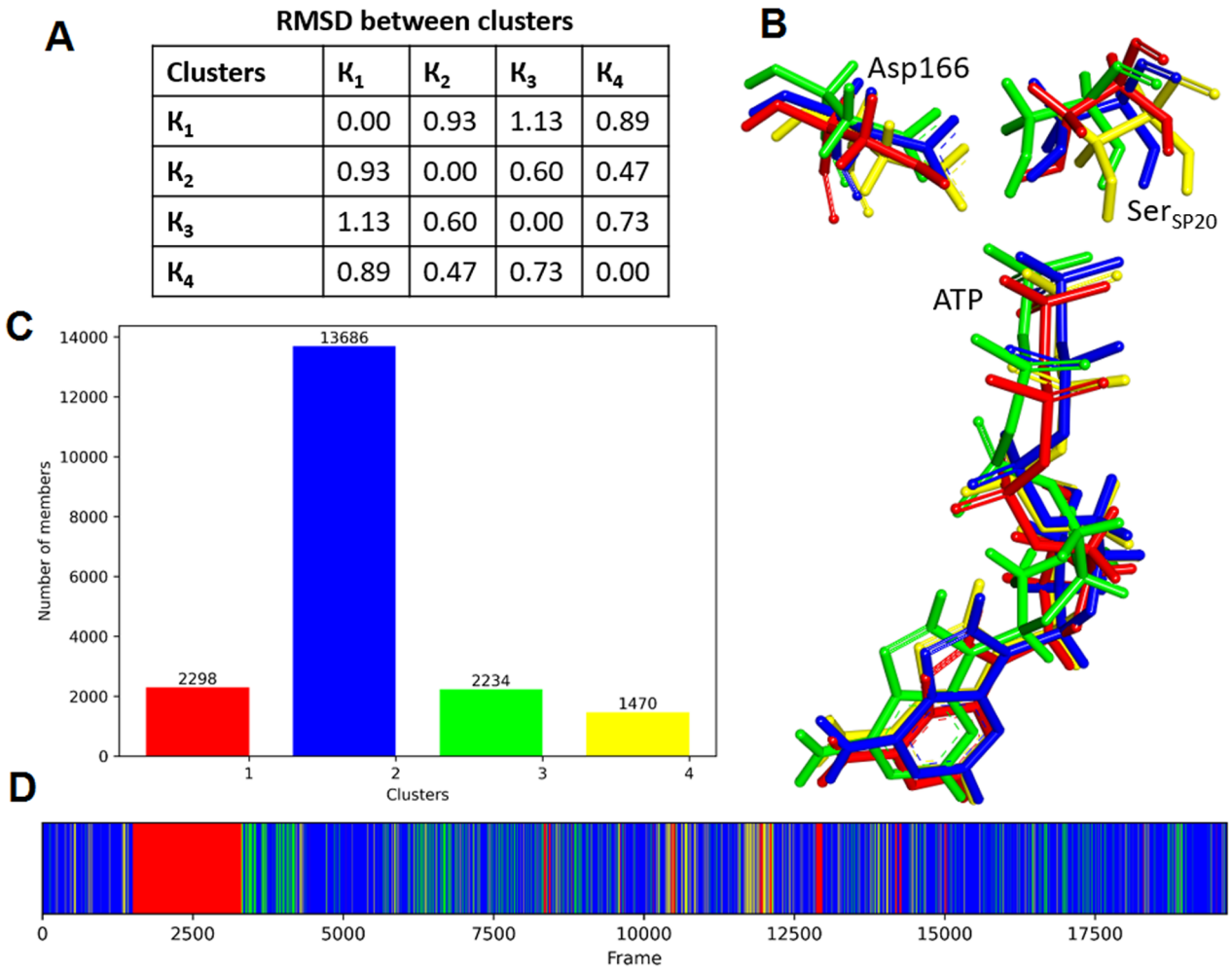

Clusters	K_1	K_2	K_3	K_4
K_1	0.00	0.93	1.13	0.89
K_2	0.93	0.00	0.60	0.47
K_3	1.13	0.60	0.00	0.73
K_4	0.89	0.47	0.73	0.00

Figure 2. A) RMSD between clusters K_1, K_2, K_3, and K_4. **B**) Alignment of representative frames from each cluster. **C**) Number of frames in each cluster. **D**) Cluster members occurrence along MD trajectories. The color version of the figure is available in the electronic version of the article.

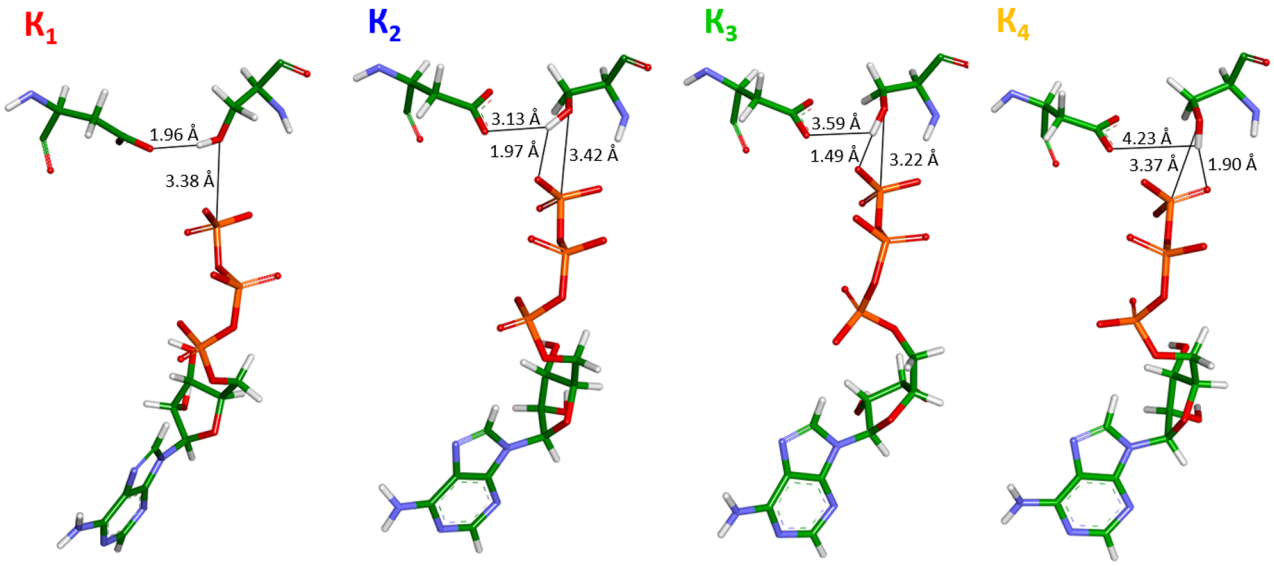

Figure 3. Representative frames corresponding to different clusters. ATP and Asp166 and Ser_{SP20} residues are depicted. The color version of the figure is available in the electronic version of the article.

Table 1. Average values and standard deviations for the distances between the proton of the hydroxy group of the serine residue of the substrate SP20 ($H(Ser_{SP20})$) and the oxygen atoms of Asp166 (O(Asp166)) and the phosphate tail (O3G(ATP) and O1G(ATP)) obtained for each cluster (K_1, K_2, K_3, and K_4)

	K_1	K_2	K_3	K_4
$H(Ser_{SP20})$-O(Asp166), Å	2.45±1.08	3.75±0.30	3.64±0.35	4.08±0.56
$H(Ser_{SP20})$-O3G(ATP), Å	3.01±0.26	1.76±0.21	1.71±0.14	2.07±0.40
$H(Ser_{SP20})$-O1G(ATP), Å	3.23±0.90	2.60±0.30	2.70±0.24	2.33±0.50

on the structure, the lone electron pair on serine oxygen is not oriented to the phosphorus atom in the K_3 cluster thus complicating the nucleophilic attack. In the K_2 cluster, the lone electron pair is oriented towards the phosphorus atom, which contributes to the initiation of the reaction. In the K_4 state, the hydrogen atom of the hydroxyl group of the serine residue forms a hydrogen bond with another oxygen of the phosphate group; however, despite the short distance of the nucleophilic attack, the nucleophile is oriented in the other direction from the phosphorus atom. In this regard, it is not necessary to consider this conformation of the enzyme-substrate complex as reactive. Most likely, the reactive conformation is K_1, since with this conformation a small distance of nucleophilic attack is observed, the hydrogen atom of the hydroxyl group forms a hydrogen bond with Asp166, which is a good proton acceptor, and the nucleophile is correctly oriented relative to the ATP phosphorus atom.

The main difference between the conformations is the location of the serine proton of the substrate ($H(Ser_{SP20})$) relative to the oxygen atoms of Asp166 (O(Asp166)) and of the phosphate tail (O3G(ATP) and O1G(ATP)). It is characterized by different distances between the corresponding atoms. In addition to determining these distances in representative structures, average values and standard deviations for distances for all structures of each cluster were obtained (Table 1). The average value of the distances $H(Ser_{SP20})$-O(Asp166) for K_1 and $H(Ser_{SP20})$-O1G(ATP) for K_4 is much higher than these values in representative structures, and a large confidence interval is also observed. In addition, comparing the average values of the distances $H(Ser_{SP20})$-O3G(ATP) and $H(Ser_{SP20})$-O1G(ATP), we can say that K_4 is a set of structures similar to representative structures for K_2, K_3, and K_4. This is also confirmed by the $H(Ser_{SP20})$-O1G(ATP) distance distribution, which is shown in Figure 4. For K_4, only 35% of the frames from the cluster respond to the representative structure. Also, frequent deviations from the representative structure are observed for K_1 (63% of frames correspond to the representative structure). The highest correspondence of cluster frames to representative structures hase been observed for K_2 and K_3 — 98% and 97%, respectively.

Additional analysis of geometry parameters was carried out. Figure 5 shows the distribution of the dihedral angle OG-CB-CA-N of the serine substrate ($Dih(Ser_{SP20})$) and the distances between the hydrogen atom of the hydroxyl group Ser_{SP20}

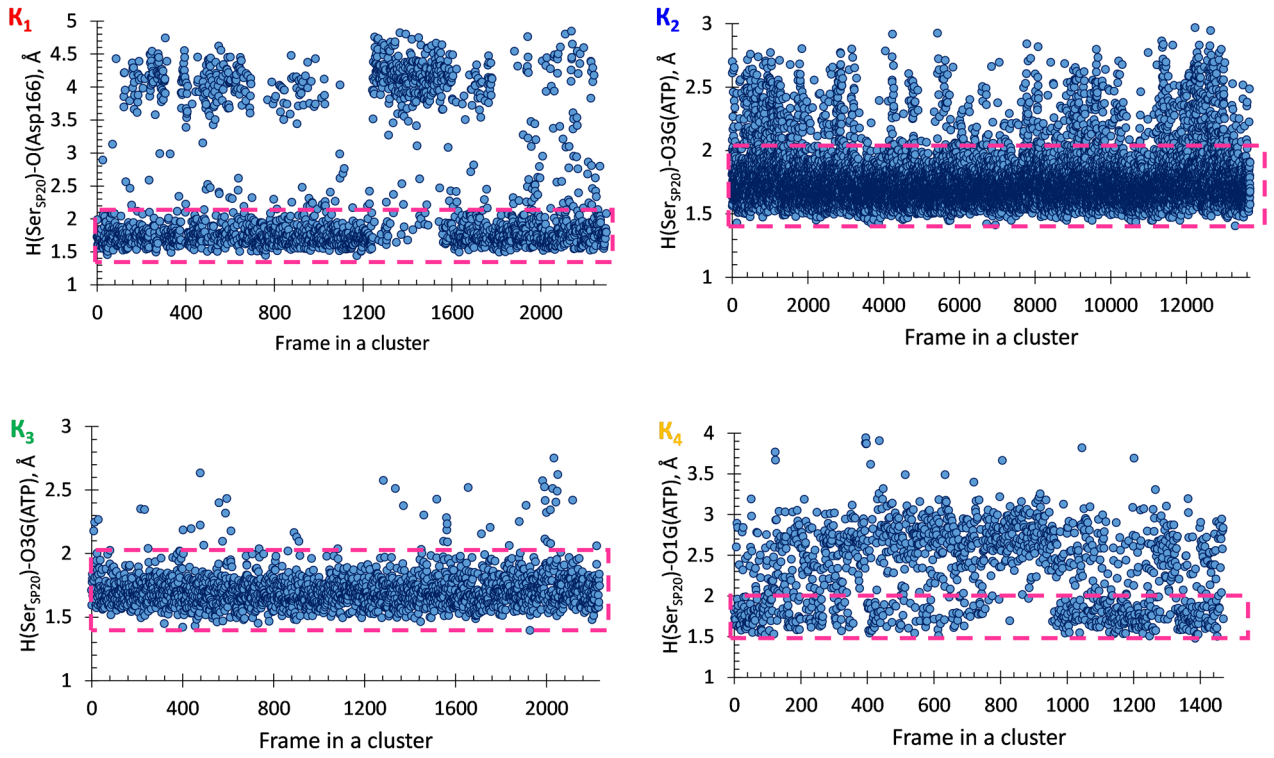

Figure 4. Distance distributions between the hydroxy group proton of the serine substrate SP20 ($H(Ser_{SP20})$) and the oxygens Asp166 (O(Asp166)) and the phosphate tail (O3G(ATP) and O1G(ATP)) obtained for each cluster (K_1, K_2, K_3, and K_4). The pink dotted line highlights the range of values corresponding to representative frames. The color version of the figure is available in the electronic version of the article.

and the oxygens of Asp166 and the γ-phosphate group of ATP. It can be seen from Figure 5A that the K_1 cluster corresponds to a region with values of $Dih(Ser_{SP20})$ from -20° to -90° and distances between the hydrogen atom and Asp166 1.4–2.5 Å. However, conformations $K_{2/3}$ and K_4 cannot be distinguished based on these geometry criteria, since in these conformations the $Dih(Ser_{SP20})$ can take values from 20° to 90°, and from -40° to -90°. Moreover, it can be seen from Figure 5B that $K_{2/3}$ correspond mainly to the positive values of the dihedral angle, whereas for K_4 those correspond almost equally to geometries with different $Dih(Ser_{SP20})$. Thus, these geometry parameters make it possible to clearly distinguish K_1 from other states. Attempts to find other geometry criteria gave at similar results. Thus, no geometry criteria were found to distinguish the conformations $K_{2/3}$ and K_4 from each other.

CONCLUSIONS

For the enzyme-substrate complex of PKA with ATP in the active site, the analysis of molecular dynamic trajectories by hierarchical clustering methods was carried out. We detected four different conformations of ATP and Asp166 and Ser_{SP20} residues in the PKA active site. These conformations differ in the position of the hydroxyl group of the serine pseudosubstrate SP20. Oxygen atoms of aspartic acid and the ATP γ-phosphate group were found as possible proton acceptors. Most likely, the most reactive conformation is the one in which the hydrogen atom of the hydroxyl group forms a hydrogen bond with Asp166 oxygen.

ACKNOWLEDGEMENTS

The research was carried out using the equipment of the shared research facilities of HPC computing resources at Lomonosov Moscow State University.

FUNDING

The study was supported by theRussian Science Foundation (project no. 23-13-00011, to M.L.).

COMPLIANCE WITH ETHICAL STANDARDS

This article does not contain any research involving humans or the use of animals as objects.

CONFLICT OF INTEREST

The authors declare no conflicts of interest.

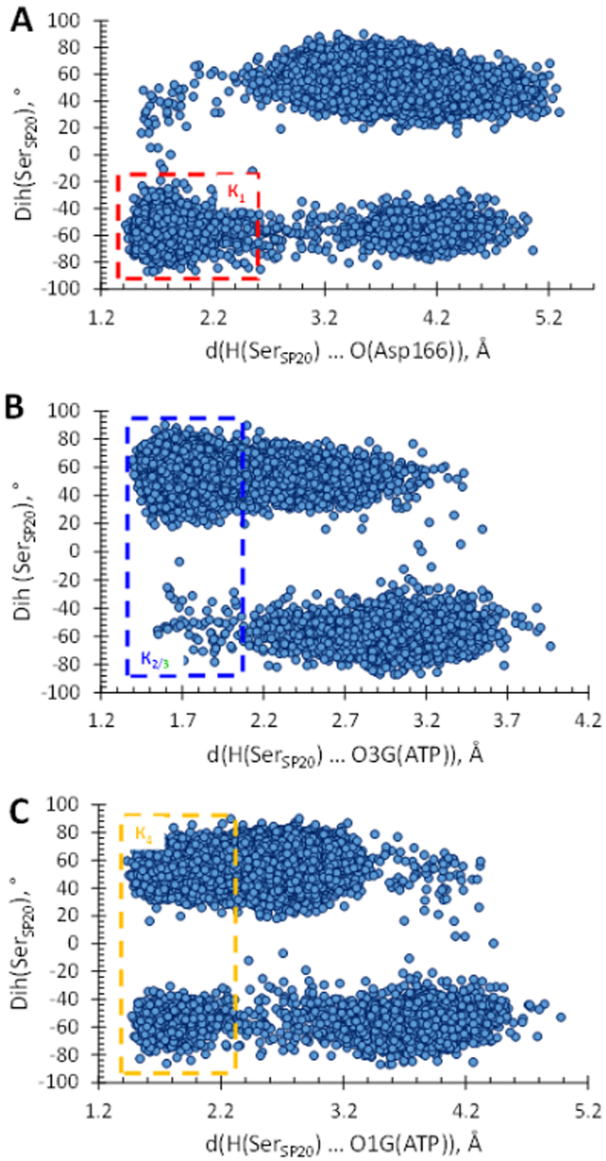

Figure 5. Dihedral angle OG-CB-CA-N of the SP20 serine residue (Dih(Ser_{SP20})) and interatomic distances between the hydrogen atom of the Ser_{SP20} hydroxyl and oxygen atoms of Asp166 (**A**) and the ATP γ-phosphate group (**B**, **C**). K_1, $K_{2/3}$, K_4 are conformations of the enzymes substrate complex of the PKA with ATP and SP20.

REFERENCES

1. *Arnsten A.F.T., Wang M.* (2020) The evolutionary expansion of mGluR3-NAAG-GCPII signaling: Relevance to human intelligence and cognitive disorders. Am. J. Psychiatry, **177**(12), 1103–1106. DOI: 10.1176/appi.ajp.2020.20101458
2. *Gasiorowska A., Wydrych M., Drapich P., Zadrozny M., Steczkowska M., Niewiadomski W., Niewiadomska G.* (2021) The biology and pathobiology of glutamatergic, cholinergic, and dopaminergic signaling in the aging brain. Front. Aging Neurosci., **13**, 654931. DOI: 10.3389/fnagi.2021.654931
3. *Pang K., Wang W., Qin J.-X., Shi Z.-D., Hao L., Ma Y.-Y., Xu H., Wu Z.-H., Pan D., Chen Z.-S., Han C.-H.* (2022) Role of protein phosphorylation in cell signaling, disease, and the intervention therapy. MedComm, **3**(4), e175. DOI: 10.1002/mco2.175
4. *Gerlits O., Waltman M.J., Taylor S., Langan P., Kovalevsky A.* (2013) Insights into the phosphoryl transfer catalyzed by cAMP-dependent protein kinase: An X-ray crystallographic study of complexes with various metals and peptide substrate SP20. Biochemistry, **52**(21), 3721–3727. DOI: 10.1021/bi400066a
5. *Johnson D.A., Akamine P., Radzio-Andzelm E., Madhusudan M., Taylor S.S.* (2001) Dynamics of cAMP-dependent protein kinase. Chem. Rev., **101**(8), 2243–2270. DOI: 10.1021/cr000226k
6. *Adams J.A.* (2001) Kinetic and catalytic mechanisms of protein kinases. Chem. Rev., **101**(8), 2271–2290. DOI: 10.1021/cr000230w
7. *Taylor S.S., Yang J., Wu J., Haste N.M., Radzio-Andzelm E., Anand G.* (2004) PKA: A portrait of protein kinase dynamics. Biochim. Biophys. Acta, **1697**(1–2), 259–269. DOI: 10.1016/j.bbapap.2003.11.029
8. *Word J.M., Lovell S.C., Richardson J.S., Richardson D.C.* (1999) Asparagine and glutamine: Using hydrogen atom contacts in the choice of side-chain amide orientation. J. Mol. Biol., **285**(4), 1735–1747. DOI: 10.1006/jmbi.1998.2401
9. *Humphrey W., Dalke A., Schulten K.* (1996) VMD: Visual molecular dynamics. J. Mol. Graph., **14**(1), 33–38. DOI: 10.1016/0263-7855(96)00018-5
10. *Phillips J.C., Braun R., Wang W., Gumbart J., Tajkhorshid E., Villa E., Chipot C., Skeel R.D., Kalé L., Schulten K.* (2005) Scalable molecular dynamics with NAMD. J. Comput. Chem., **26**(16), 1781–1802. DOI: 10.1002/jcc.20289
11. *Best R.B., Zhu X., Shim J., Lopes P.E.M., Mittal J., Feig M., MacKerell A.D.* (2012) Optimization of the additive CHARMM all-atom protein force field targeting improved sampling of the backbone ϕ, ψ and side-chain χ_1 and χ_2 dihedral angles. J. Chem. Theory Comput., **8**, 3257–3273. DOI: 10.1021/ct300400x
12. *Vanommeslaeghe K., Hatcher E., Acharya C., Kundu S., Zhong S., Shim J., Darian E., Guvench O., Lopes P., Vorobyov I., Mackerell A.D.* (2009) CHARMM general force field: A force field for drug-like molecules compatible with the CHARMM all-atom additive biological force fields. J. Comput. Chem., **31**, 671–690. DOI: 10.1002/jcc.21367
13. *Jorgensen W.L., Chandrasekhar J., Madura J.D., Impey R.W., Klein M.L.* (1983) Comparison of simple potential functions for simulating liquid water. J. Chem. Phys., **79**, 926–935. DOI: 10.1063/1.445869
14. *Quigley D., Probert M.I.J.* (2004) Langevin dynamics in constant pressure extended systems. J. Chem. Phys., **120**(24), 11432–11441. DOI: 10.1063/1.1755657
15. *Martyna G.J., Tobias D.J., Klein M.L.* (1994) Constant pressure molecular dynamics algorithms. J. Chem. Phys., **101**(5), 4177–4189. DOI: 10.1063/1.467468
16. *Feller S.E., Zhang Y., Pastor R.W., Brooks B.R.* (1995) Constant pressure molecular dynamics simulation: The Langevin piston method. J. Chem. Phys., **103**(11), 4613–4621. DOI: 10.1063/1.470648
17. *Tubiana T., Carvaillo J.-C., Boulard Y., Bressanelli S.* (2018) TTClust: A versatile molecular simulation trajectory clustering program with graphical summaries. J. Chem. Inf. Model., **58**(11), 2178–2182. DOI: 10.1021/acs.jcim.8b00512
18. *Ward J.H. Jr.* (1963) Hierarchical grouping to optimize an objective function. J. Am. Stat. Assoc., **58**, 236–244. DOI: 10.1080/01621459.1963.10500845

Received: 30. 10. 2024.
Revised: 17. 11. 2024.
Accepted: 19. 11. 2024.

КОНФОРМАЦИОННАЯ ДИНАМИКА ФЕРМЕНТ-СУБСТРАТНОГО КОМПЛЕКСА ПРОТЕИНКИНАЗЫ А С ПСЕВДОСУБСТРАТОМ SP20 И АДЕНОЗИНТРИФОСФАТОМ

Т.И. Мулашкина[1]*, М.С. Леонова[1,2], М.Г. Хренова[1,3]

[1]Московский государственный университет имени М.В. Ломоносова, химический факультет,
119991, Москва, Ленинские горы, 1, стр. 3; *эл. почта: mulashkinati@my.msu.ru
[2]Институт биохимической физики им. Н.М. Эмануэля Российской академии наук,
119334, Москва, ул. Косыгина, 4
[3]Институт биохимии им. А.Н. Баха, Федеральный исследовательский центр
“Фундаментальные основы биотехнологии” Российской академии наук,
119071, Москва, Ленинский пр-т, 33, стр. 2

Реакция фосфорилирования, катализируемая ферментом протеинкиназой А (ПКА), является одной из ключевых в работе глутаматергической системы — базовой системы памяти. Анализ динамического поведения фермент-субстратного комплекса позволяет во многом судить о дальнейшем механизме ферментативной реакции. По результатам классических молекулярно-динамических расчётов с последующей иерархической кластеризацией показано, что наиболее предпочтительным акцептором протона в ходе реакции фосфорилирования ПКА является карбоксильная группа аминокислотного остатка Asp166, однако акцептором также может выступать γ-фосфатная группа АТР.

Полный текст статьи на русском языке доступен на сайте журнала (http://pbmc.ibmc.msk.ru).

Ключевые слова: протеинкиназа А; молекулярная динамика; конформации; фермент-субстратный комплекс; АТР

Финансирование. Работа выполнена при поддержке Российского научного фонда (проект 23-13-00011, участник М.Л.).

Поступила в редакцию: 30.10.2024; после доработки: 17.11.2024; принята к печати: 19.11.2024.